Manuscript Details

Manuscript number	SUBMIT2IJMS_2018_3659_R1
Title	An Experimental and Numerical Study of a CoNiCrAlY Coating Using Miniature Specimen Testing Techniques
Article type	Research Paper

Abstract

Small punch tensile (SPT) tests have been carried out for a CoNiCrAlY coating at room temperature (RT), 500°C and 700°C. Highly re-producible results have been obtained for SPT at 700°C while the formation of early cracking at lower temperatures tends to compromise the repeatability of the tests. An alternative novel miniature specimen testing method has been developed and used for the miniature tensile tests of the CoNiCrAlY coating in the same temperature range. Good agreements have been achieved between the SPT and miniature tensile testing results regarding the ductile to brittle transition temperature (DBTT). Excellent repeatability has been achieved over the full range of the temperature for the miniature tensile tests. An inverse approach has been developed and used to extract the mechanical properties of the material from the miniature tensile tests, using a temperature-dependent Johnson-Cook model. Finite element (FE) modelling of the SPT tests, including damage evolution, has been carried out using the extracted material properties to give comparable predictions of the SPT testing results, such as the load-displacement curves and the approximate locations of the fracture failures.

Keywords	CoNiCrAlY coating; miniature tensile test; small punch tensile test; high temperature properties; inverse method; ductile-to-brittle transition
Manuscript category	SOLID MECHANICS

Corresponding Author	Wu Wen
Order of Authors	Wu Wen, George A Jackson, Hezong Li, Wei Sun

Submission Files Included in this PDF

File Name [File Type]

Cover Letter.docx [Cover Letter]

Reply to editor.pdf [Response to Reviewers]

Highlights.docx [Highlights]

IJMS_15-11-2018 [Revised & Marked].docx [Manuscript File]

To view all the submission files, including those not included in the PDF, click on the manuscript title on your EVISE Homepage, then click 'Download zip file'.

Dear Editor-in-Chief,

An Experimental and Numerical Study of a CoNiCrAlY Coating Using Miniature Specimen Testing Techniques

W. Wen, G.A. Jackson, H. Li, W. Sun

We are submitting the above manuscript to *International Journal of Mechanical Sciences* for your kind consideration and assessment.

Thank you very much,

Yours sincerely,

Wu Wen

Email: wenwu.gm2011@gmail.com

Dear Editor,

We extremely appreciate the referees' comments and suggestion on this manuscript. All the comments have been carefully addressed accordingly. The modifications have been highlighted in yellow and blue colours respectively, in relation to the comments from reviewer 1 and reviewer 2 in the marked version of revised manuscript (IJMS_15-11-2018 [Revised & Marked].docx).

Thank you very much.

Regards,

Corresponding Author

29/03/2019

Comments from the editors and reviewers:

-Reviewer 1

The authors have written an interesting manuscript that discusses the relationship between miniaturised uniaxial tensile testing and small punch tensile testing. The research is scientifically sound and well corroborated with finite element models. Prior to submission, the following points must be addressed:

Introduction line 10 - should read coating's microstructures
The text has been corrected (**1.**).

Introduction - When referring to the CoP, also need to reference the following paper: European standard on small punch testing of metallic materials, Bruchhausen, M., Austin, T. et al, American Society of Mechanical Engineers, Pressure Vessels and Piping Division (Publication) PVP, 2017
The reference has been included (**[15]**) and the order of the other references has been updated accordingly.

The authors need to state why a displacement rate of 1um/s was chosen for SPT testing.
This rate is the resolution of the machine (**3.1**). This has been mentioned in the text.

The authors need to state why a disc thickness of 400um was chosen.
The thickness of 0.4mm was chosen to more accurately reflect the thickness of bond coats used in service (around 0.2 mm) whilst still being within the limits of the equipment and close to the standard thickness of 0.5mm. This has been mentioned in the text (**3.1**).

All dimensions of the test configuration are not consistent with those stated in the European CoP - what is the reason for this?
The punch radius was mistakenly stated to be 1mm and it has been corrected to be 1.25mm (**3.1**). The diameters of the specimen (8mm) and the receiving hole (4mm) are also consistent with the European standard. This has been corrected in the text (**3.1**). Since the thickness of the specimen was different from the standard, the statement 'All tests were carried out in accordance with the CEN workshop agreement' has been deleted in the text (**3.1**).

The authors need to state the clamping force on the disc as this can have a significant influence on the mechanical response.
The specimens were fixed to avoid movement during the tests, but the clamping force was not measured. This has been pointed out in the discussion section as a way to improve the current SPT testing results (**7.**).

Section 3.2 - The authors state that the reason for the drops on the load-displacement curve is cracking - this needs to be supported by a reference or relevant image of the specimen at this stage
References have been included (**[9, 26]**).

Figure 2 - Alternative colours, line style need to be used as no differentiation can be made between the different series.

Figure 2 caption needs to be corrected
Figure 2 has been modified as suggested, the text has been changed accordingly (**3.2**).

Table 1 would benefit from the addition of strain to failure and UTS results
The suggested data have been included in Table 1 (**4.2.1**).

-Reviewer 2

It is a well planned and executed research, the writing is good, and the paper should be published with minor corrections such as:

1. Small punch test: how many tests have been repeated?

Tests were repeated three times at each temperature. This has been mentioned in the text (**3.1**).

2. Figure 2(a), line pattern to change so that the difference between RT and 500 deg C is clear?

Figure 2 has been modified (**3.2**).

3. MATLAB code should be referenced?

Reference has been included for MATLAB (**[31]**).

4. The value of selected minimum step size, and the threshold value for the termination of optimisation?

These values have been specified (**5.2**).

5. In discussion section, there are a number of statements made, could you please make them cleaner, by adding the reference or it is speculative by the current authors.

Clarification and modifications have been added to the discussion section (**7.**).

Highlights

- Ductile-to-brittle transition was revealed by small punch and miniature tensile tests
- Miniature tensile tests demonstrated high consistency and repeatability
- An inverse method developed to determine the temperature-dependent mechanical properties
- Finite element modelling was carried out to predict damage evolution and fracture

An Experimental and Numerical Study of a CoNiCrAlY Coating Using Miniature Specimen Testing Techniques

W. Wen[1,*], G.A. Jackson[1], H. Li[2,*], W. Sun[1]

[1]Faculty of Engineering, University of Nottingham, University Park, Nottingham NG7 2RD, UK

[2]School of Mechanical and Equipment Engineering, Hebei University of Engineering, Handan, 056038, China

*Correspondence: wenwu.gm2011@gmail.com; Tel.: +44-752-697-3730

Abstract

Small punch tensile (SPT) tests have been carried out for a CoNiCrAlY coating at room temperature (RT), 500°C and 700°C. Highly re-producible results have been obtained for SPT at 700°C while the formation of early cracking at lower temperatures tends to compromise the repeatability of the tests. An alternative novel miniature specimen testing method has been developed and used for the miniature tensile tests of the CoNiCrAlY coating in the same temperature range. Good agreements have been achieved between the SPT and miniature tensile testing results regarding the ductile to brittle transition temperature (DBTT). Excellent repeatability has been achieved over the full range of the temperature for the miniature tensile tests. An inverse approach has been developed and used to extract the mechanical properties of the material from the miniature tensile tests, using a temperature-dependent Johnson-Cook model. Finite element (FE) modelling of the SPT tests, including damage evolution, has been carried out using the extracted material properties to give comparable predictions of the SPT testing results, such as the load-displacement curves and the approximate locations of the fracture failures.

Keywords: CoNiCrAlY coating; miniature tensile test; small punch tensile test; high temperature properties; inverse method; ductile-to-brittle transition

Nomenclature

Symbol	Definition	Unit
A	Yield stress at reference temperature (Johnson-Cook constitutive model)	MPa
B, C, m	Johnson-Cool constitutive constants	
E	Elastic modulus	GPa
P	Force	N
T, T_r, T_m	Temperature, reference temperature, melting temperature	°C, K
ε	Strain	
$\dot{\varepsilon}, \dot{\varepsilon}_0$	Strain rate, reference strain rate	s^{-1}
σ, σ_y	Stress, yield stress	MPa
Δ	Displacement	mm

1. Introduction

Many engineering applications, such as power plants, chemical plants, gas turbines and aero-engines, operate at elevated temperatures in order to achieve high thermal efficiency and reduce emissions. Thermal barrier coatings (TBC's) are widely used in such applications to protect the engineering components from the high temperature environment **[1]**. The thermal protection is achieved through a ceramic top coat that is commonly adhered to the substrate through a metallic bond coat **[1, 2]**. Understanding the high temperature behaviour of TBC's is crucial for evaluating and predicting the integrity and reliability of the engineering components. Standalone investigations into the metallic bond coats are a necessary step in order to understand the behaviour of the multi-material TBC system. CoNiCrAlY alloys have been widely used as bond coats for TBC systems because of low cost, improved control of composition and the feasibility to tailor the coating's microstructures **[3, 4]**. A number of previous studies have investigated CoNiCrAlY coatings but have typically focused on oxidation behaviour with little attention given to the mechanical properties of the coatings **[5-7]**. This, in part, is because conventional mechanical testing techniques, such as uniaxial tensile testing, are not suitable for evaluating the mechanical properties of thin CoNiCrAlY bond coats, which are typically around 200 μm thick in a TBC **[1]**. Some types of small specimen testing techniques, such as the small ring tests **[8]**, the small punch tensile (SPT) test and the small punch creep (SPC) test **[5, 9, 10]**, have clear advantages over conventional testing techniques due to the ability to employ thin specimens with similar thicknesses to bond coats used in TBC's **[11].** A number of recent studies have demonstrated the suitability of the SPC and SPT tests for determining the mechanical properties of bond coats **[9, 10, 12, 13]**. A code of practice has been developed in Europe for the standardisation and interpretation of the SPT and SPC tests **[14, 15].** Despite this, it is still difficult to accurately interpret the output data, i.e. the load-displacement curves from the SPT and the displacement-time curves from the SPC tests, due to the complex physical nature of the nonlinear behaviours involved, e.g. large local plastic strain, large deformation, pre-straining during loading, early cracking and contact friction evolution, etc.

Efforts have been made by researchers to develop miniaturised tensile specimens **[16-20]**. Most of those studies are carried out on typical metal alloys, but much less have been applied

to coatings. For the thermally sprayed coatings, the presence of porosity is generally expected, though it can be reduced by heat treatments **[9, 18]**. Due to the miniaturised size of the specimen, the local heterogeneity induced by the existence of porosity or other defects could have non-negligible influences on the testing results and could lead to significant data scatters. Similarly, the effects of surface oxidation could also be amplified by the miniaturised size of the specimens.

Inverse methods have been employed in many studies to characterise material behaviours using various testing techniques, such as micro-indentation tests **[21, 22]**, three-point bending (TPB) tests **[23]**, and SPT tests **[24]**. One of the advantages of inverse methods is that it is easy to implement, even for investigators with limited theoretical knowledge of the testing techniques. Also, most factors of influence can be taken into considerations by inverse methods since they are entirely based on the experimentally measurable quantities. However, it also means that the validity of inverse methods greatly depends on the accuracy and consistency of the physical experimental data. It should be noted that inverse methods could incur high computation cost, especially when complex finite element (FE) analyses are involved.

The current study investigates the high temperature mechanical properties of a CoNiCrAlY coating using the SPT and miniature tensile tests. An inverse method is developed and used to extract the mechanical properties of the coating with a modified Johnson-Cook constitutive model **[25]**, which takes into account of the temperature effects on the plastic stress-strain behaviours of materials. The extracted material properties have been used for FE modelling of the SPT tests of the coating material with damage evolution.

2. Materials, HVOF Thermal Spraying and Heat Treatment

The coating material used in the miniature tensile tests was produced by high velocity oxygen fuel (HVOF) thermal spraying using a commercially available powder known as Praxair CO-210-24 with the following composition: Co-31.7Ni-20.8Cr-8.1Al-0.5Y (wt.%). The powder had a size range of -45+20 μm with a chemically analysed oxygen content of 0.037 wt.%. The coating was deposited onto mild steel substrates of dimensions 60 × 25 × 1.8 mm using a Met Jet III liquid fuel HVOF gun. The spraying procedure is detailed elsewhere **[26]**. The mild steel substrate was not grit blasted to aid debonding after spraying. The coating was sprayed to a thickness of approximately 600 μm and then debonded from the mild steel by bending around a mandrel to produce free standing coatings. Vacuum heat treatment was carried out on free-standing samples at 1100°C for two hours in an Elite Thermal Systems TVH12 vacuum tube furnace held at approximately 10^{-9} bar followed by furnace cooling to room temperature over a period of 6 hours. This treatment was applied in order to approximately replicate the initial heat treatment given to bond coats during the manufacture of thermal barrier coatings. This type of heat treatment has been shown to reduce the porosity commonly present within sprayed coatings and allow the precipitation of secondary phases **[10, 26]**. Specimens for both the SPT and miniature tensile tests were cut from the heat-treated coating by electro-discharge machining. They were ground down from the as-deposited thickness to a final thickness of 500 μm on 1200 grade silicon carbide paper. The final thickness was controlled to within ± 5 μm as measured by a digital micrometer and both surfaces had the same finely ground surface finish.

3. Small Punch Tensile Testing

3.1. Small Punch Tensile Testing Method

Displacement-controlled SPT tests were performed on a Tinius Olsen H5KS single column materials testing machine at the displacement rate of 1 μm/s (maximum resolution of the machine) at RT, 500°C and 700°C. Three repeat tests were conducted at each temperature. Similar SPT tests were carried out on the same testing rig by Jackson et al **[9]**. **Figure 1** shows a schematic of the SPT testing rig. The diameter and thickness (t) of the disk specimen were 8 mm and 0.4 mm, respectively. The thickness of 0.4mm was chosen to more accurately reflect the thickness of bond coats used in service (around 0.2 mm) whilst still being within the limits of the equipment. The radius of the punch head (a) was 1.25 mm. The radius of the receiving hole (a_p) was 2 mm. The specimen was clamped by the clamping nut (b) which was screwed onto the lower die (c). A clamping disc (d) was used to eliminate friction between the clamping nut and specimen (e). The displacement of the punch head was measured by two linear variable displacement transducers (LDVT's) placed at the base plate (f). The specimens were heated to temperature in a three tier, 3 Kw furnace and held at temperature for 1 hour before application of the load. The temperature was measured by a thermocouple located at (g) and the temperature fluctuation was controlled within ±1°C.

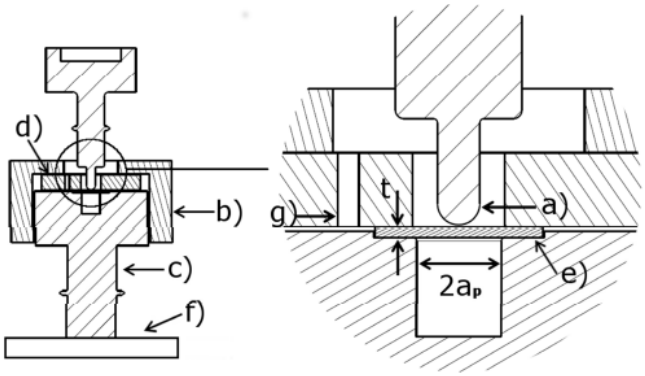

Figure 1. Schematic of the SPT testing rig. Figure reproduced from **[9].**

3.2. Results of Small Punch Tensile Tests

The representative force-displacement curves obtained from the SPT tests on the CoNiCrAlY coating at RT, 500°C and 700°C are shown in **Figure 2(a).** At RT and 500 °C the curves are predominately linear in the early stage, indicating similar elastic bending deformation, but exhibit sharp load-drops followed by clear changes in behaviour. These load-drops are indicative of cracking in the specimen **[9, 26]**. Beyond cracking, the consistency of the force-displacement curves was significantly reduced, demonstrating non-linear tensile behaviour after cracking occurred.

At 700°C, the load-displacement curves are almost identical for the repeated tests. It should also be noted that there is no early load drop at 700°C, indicating that there is no early crack initiation. These differences between the results at 700°C and the lower temperatures suggest that the material behaviour varied significantly across the temperature range. The ductility of a coating material can be defined as the strain required for crack initiation **[27]**. It is difficult to determine a representative strain for the SPT testing, therefore the total energy absorbed up to the first load drop (crack initiation) or the maximum load if no early cracking was used to quantify the ductility of the material. **Figure 2(b)** shows the total work done by the punch before cracking or maximum load during the SPT tests (calculated as the average integrations of the load-displacement curves) as a function of temperature. The increase in the absorbed energy is relatively small from RT to 500°C while it increased drastically from 500 to 700°C. This

phenomenon indicates that the coating experienced a brittle to ductile transition between 500 and 700°C. A similar transition was reported by Jackson et al **[9]**, where the ductile-to-brittle transition temperature (DBTT) is found to be between 500-700°C.

The fracture surfaces of the failed SPT test specimens were examined to better understand the change in behaviour between 500 and 700°C. The fracture at 500°C was characterised by a star-like cracking pattern in the centre of the specimen, **Figure 3(a)**, known to be associated with brittle failure **[27, 28]**. At 700°C, fracture was characterised by circumferential cracking, as seen in **Figure 3(b),** which is known to be associated with ductile failure **[9, 27, 29].** These findings indicated that the DBTT of the current HVOF coating manufactured from Praxair CO-210-24 was between 500-700°C, in agreement with that reported in **[9]**.

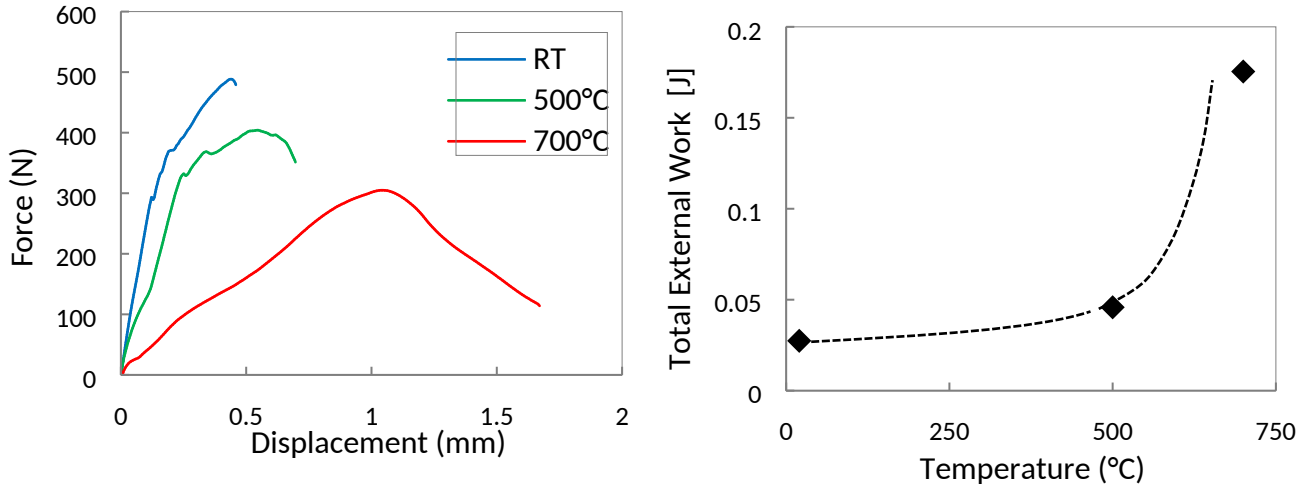

(a) (b)

Figure 2. (a) Load-displacement curves and (b) total external work as a function of temperature (b) for SPT tests between RT and 700°C.

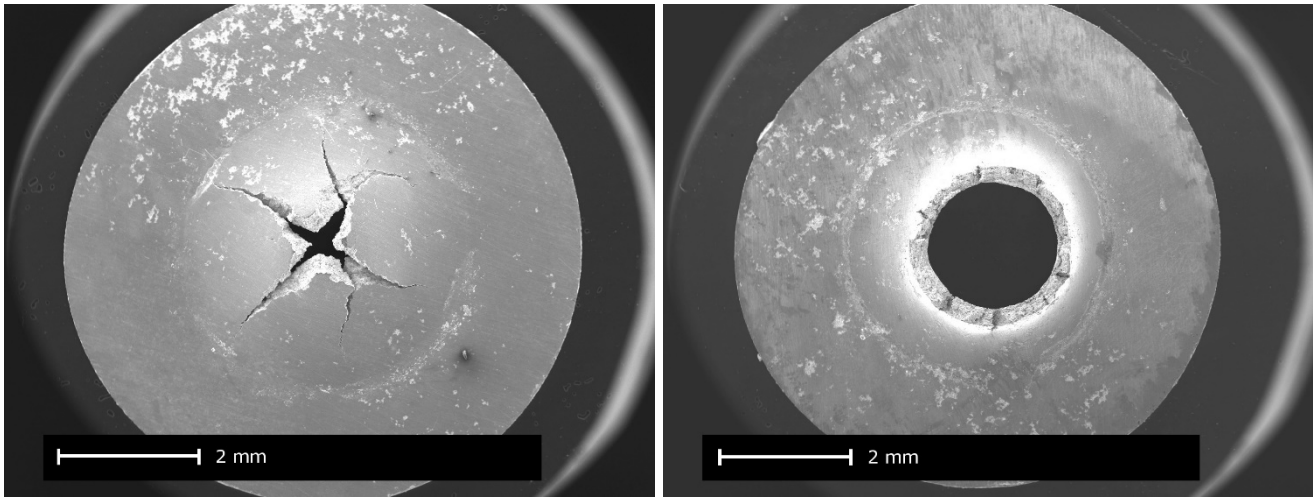

(a) (b)

Figure 3. SEM images of fracture patterns following SPT testing at (a) 500°C and (b) 700°C. The 500 °C specimen exhibits a star-like cracking pattern in the centre of the specimen whereas the 700 °C specimen exhibits circumferential cracking.

4. Miniature Tensile Testing

4.1. Miniature Tensile Testing Method

The miniature tensile tests were carried out using the same Tinius Olsen H5KS single column materials testing machine described in **3.1**. The geometry and dimensions of the miniature testing specimen are shown in **Figure 4 (a). Figure 4 (b)** shows the loading assembly and how the miniature specimen was clamped and mounted to the machine. The loading assembly parts were made of a high temperature nickel-based superalloy, Nimonic 115. The specimen was clamped at both ends by specially manufactured clamps with machined surface features to increase the friction between the clamp and specimen. The displacement was measured by two LDVT's connected to both sides of the loading parts of the machine. The mounted specimens were heated in a 3 tier, 3 Kw furnace except for the RT test. Tensile tests were carried out at RT, 500°C, 600°C and 700°C. Multiple tests were carried out at each temperature to verify the consistency of the testing method. The loading process was controlled at the constant displacement rate of 0.006 mm/s (to achieve a strain rate of 0.001 /s, approximately). It had been verified by preliminary tests that the results of the tensile tests had very low sensitivity to the loading rate between 0.0006 mm/s and 0.06 mm/s. The torque applied to the clamps was adjusted to 0.5 Nm in order to avoid inducing any cracking in the specimen while providing sufficient clamping force to avoid slipping.

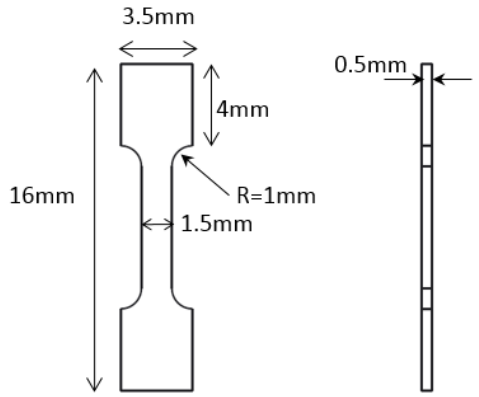

(a)

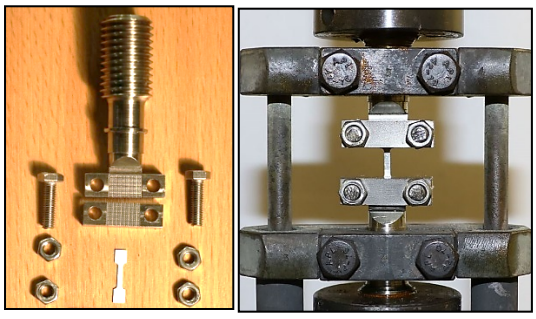

(b)

Figure 4. (a) Dimensions of the miniature specimen and (b) the loading assembly and the mounted specimen.

4.2. Results of Miniature Tensile Tests

4.2.1. Mechanical Behaviour

The engineering stress-strain curves, estimated from the loading force, original cross-section area and loading direction displacement, obtained from the miniature tensile tests are shown in **Figure 5**. It should be noted that the displacement measurements were taken at the clamped ends (outside the gauge length region) because it is very difficult to fit a gauge into the very limited space. Therefore, the measured displacement was different from the actual displacement of the gauge length area. An equivalent gauge length (EGL), $L_{EGL} = \beta L_o$(β is a constant decided by the geometry of the specimen and the loading conditions, and $L_o$is the original gauge length), was estimated based on FE analyses, where $\beta \approx 1.2$. The repeatability of the multiple tests carried out at each temperature, RT, 500°C, 600°C and 700°C, was very good. It is clear that the ultimate tensile stress (UTS) decreases as temperature increases from RT to 700°C. At and below 600°C, there was only the elastic deformation phase and the strain-hardening phase, but no clear sign of material softening before failure, while there was a clear phase of material softening before reaching failure at 700°C. The observed material softening at 700°C might be due to the recrystallisation of the material at elevated temperature. A notable phenomenon observed in the SPT tests was the sudden load drop at low strains, which indicated the formation of early cracking at and below 500°C (shown in **Figure 2(a)**). No sign of early cracking was found in the miniature tensile tests, indicating that it is an effective mechanical testing technique for this coating material at a wide range of temperature, despite the ductile-to-brittle transition of the material.

The estimated mechanical properties of this coating material are presented in **Table 1**. Generally, the elastic modulus and the yield stress decrease with increasing temperature. Regarding the failure strain, the increase from RT to 600°C is relatively small while it increases significantly from 600°C to 700°C. These transitions are shown more clearly in **Figure 6.** The intersection of the UTS and failure strain curves, shown in **Figure 6 (a)**, indicates that the DBTT to be near 650°C. **Figure 6 (b)** shows the estimated tensile toughness, calculated as the area under the stress-strain curves, and the estimated elastic modulus as a function of temperature. It is clear that the tensile toughness of this coating material remained relatively constant between RT and 600°C while it increased by nearly 300% when temperature was increased to 700°C. Again, this is another indication of ductile-to-brittle transition. Similarly, the temperature effect on the elastic modulus was not significant at temperature between RT and 500°C while the elastic modulus dropped by over 60% when temperature was increased from 500°C to 700°C. Those findings were in very good agreements with the results from the corresponding SPT tests present in section **3.2**.

Regarding the deformation of the failed specimens, there was no visible necking, which makes the engineering stress-strain close to the true stress-strain, in all the miniature tensile tests even until the failures of the specimens at all temperatures. These facts indicate that the stress-strain curves obtained from the miniature tensile tests are relatively complete and reliable. Compared to the SPT testing technique, this miniature specimen testing method also has the advantage that the interpretation of the experimental results is relatively straightforward, i.e. the stress-strain relationships can be conveniently obtained from the force-displacement data.

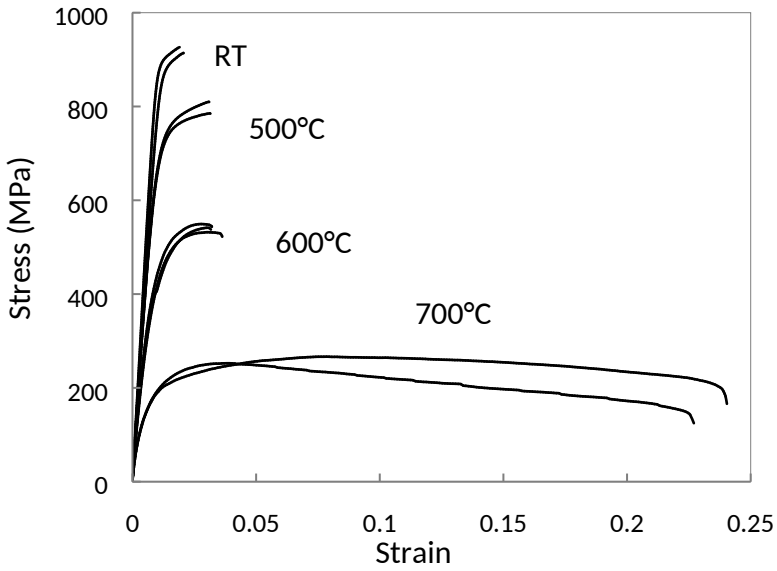

Figure 5. Stress-strain curves obtained from the miniature tensile tests on the CoNiCrAlY coating at temperatures from RT to 700°C.

Table 1 Mechanical properties of the CoNiCrAlY coating estimated from the stress-strain curves.

	RT	500°C	600°C	700°C
E (GPa)	83.6	75.6	47.5	40.0
σ_y *(MPa)*	850	750	450	100
Strain to Failure	0.021	0.031	0.036	0.235
UTS (MPa)	933	809	549	252

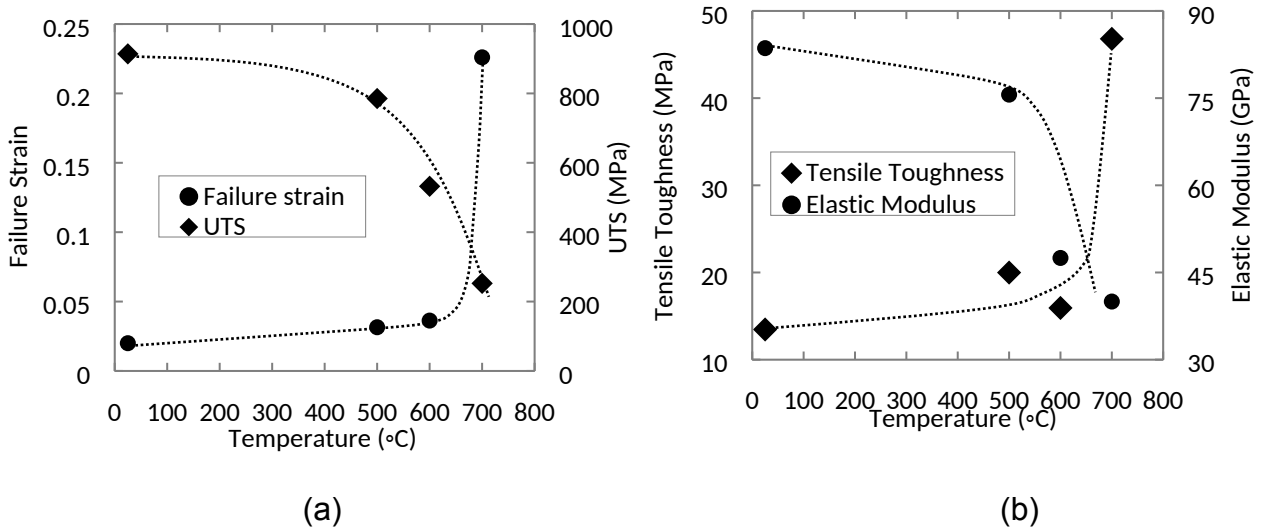

Figure 6. (a) The failure strain and UTS and (b) the tensile toughness and elastic modulus as functions of temperature for miniature specimen tensile tests between RT and 700°C.

4.2.2. Microscopic Fracture Behaviour

Secondary electron (SEM) images showing the fracture surfaces of the miniature tensile tests specimens tested at 500°C and 700°C are shown in **Figure 7.** At 500°C (**Figure 7 (a-b)**) there are noticeable concave or convex features, which are relatively smooth and approximately up to 30 to 40 μm in size. These features are identified as powder particles which indicates brittle failure occurred along the powder particle boundaries. In contrast, no such features are identified on the fracture surface of the specimen tested at 700°C, as shown in **Figure 7 (c-d)**. The 700°C fracture surface consists of small, rounded surface features that indicate ductile failure.

The fracture surfaces of the miniature tensile testing specimens for 500°C and 700°C demonstrate a clear change in fracture behaviour between 500-700°C. This verifies the ductile to brittle transition indicated by the stress-strain curves and the low magnification SEM images of the fracture surfaces obtained from the SPT tests (**Figures 2 and 3**).

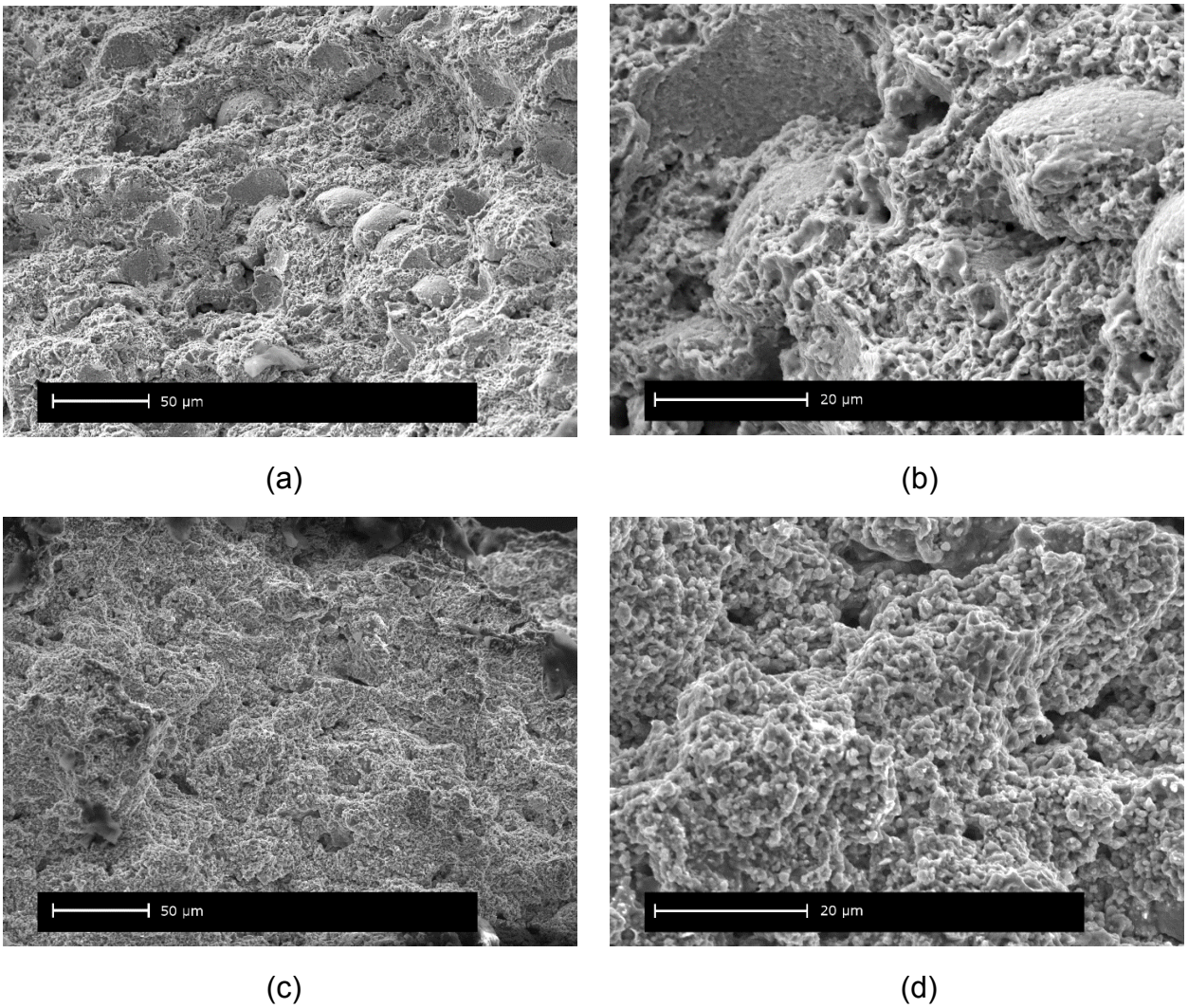

Figure 7. Secondary electron images showing the fracture surfaces of the coating specimens following miniature specimen tensile tests at (a-b) 500°C and (c-d) 700°C.

5. Inverse Approach

5.1. Material Constitutive Model

To characterise the mechanical behaviours of the coating material, an elastic-plastic material model was employed under the uniaxial conditions. A simple Hooke's law was applied for the elastic deformation, i.e. $\sigma = E\varepsilon$, where σ is the stress, ε is the strain and E is the elastic modulus. For the plastic deformation, the Johnson-Cook constitutive model **[24]** was used to describe the strain hardening behaviour, taking into account of the effects of temperature. The original Johnson-Cook model is expressed as follows:

$$\sigma = \left(A + B\varepsilon^{n}\right)\left(1 + C\ln \dot{\varepsilon}^{*}\right)\left(1 - T^{*m}\right) \quad (1)$$

$$\dot{\varepsilon}^{*} = \frac{\dot{\varepsilon}}{\dot{\varepsilon}_0} \quad (2)$$

$$T^{*} = \frac{T - T_r}{T_m - T_r} \quad (3)$$

where A is the yield stress at the selected reference temperature, T_r, B is the strain hardening coefficient, n is the strain hardening exponent, C is the material constant for strain rate hardening, m is the material constant for thermal softening exponent, $\dot{\varepsilon}$ is the applied strain rate, $\dot{\varepsilon}_0$ is the reference strain rate, T is the applied temperature and T_m is the melting temperature of the material (temperatures are in unit of K). The melting temperature of the CoNiCrAlY coating material is approximately 1350°C or 1623K (the powder used to prepare the coating was obtained from Praxair, powder code CO-210-24).

In this study, the strain rate hardening was neglected. The Johnson-Cook constitutive equation, Eq (1), was simplified as follows:

$$\sigma = \left(A + B\varepsilon^{n}\right)\left(1 - T^{*m}\right) \quad (4)$$

It should be noted that the temperature effects on elastic properties are not included by the Johnson-Cook constitutive model.

5.2. Inverse Method Procedures

An inverse method was developed to extract the Johnson-Cook constitutive properties from the miniature tensile tests on the CoNiCrAlY coating. **Figure 8** shows the flowchart of the inverse method. The experimental data obtained from the miniature tensile tests are supplied as the target values in the form of load (*P*)-displacement (Δ) curves. An initial guess of the Johnson-Cook constitutive properties is provided to start the iterative algorithm. This initial guess can be obtained by performing a numerical function fitting based on the Johnson-Cook constitutive equations and the stress-strain data obtained from a similar material. A nonlinear optimisation function (fminsearch) based on the optimisation toolbox in the commercial code Matlab R2015a **[31]** was employed, cooperated with a FE model of the miniature specimen, to obtain FE predictions for the corresponding miniature tensile tests and calculate the total differences compared to the experimental data. The FE results were extracted using a Python script constructed for the FE model built using the commercial code Abaqus 6.14-1. An objective function was constructed to obtain the minimum value of the total differences between FE predictions and experimental results. The inverse algorithm stops automatically once the objective function value is minimised to be smaller than a user-defined threshold value. It should

be noted that the constitutive constants (*A, B, n* and *m*) are in very different orders. These constants need to be scaled similar orders, based on a selected minimum step size, to ensure that the optimisation algorithm works efficiently on all constitutive constants. The ratio of the minimum step size (5×10^{-5}) to the magnitude of the scaled constant (1×10^{-3}) is crucial, e.g. if the step size is too small then the optimisation might not progress efficiently or might not able to converge close to the target conversely. A selected number of data points were taken from each part of the load-displacement curve, i.e. more data points are taken from the curved part than the linear part (the Johnson-Cook constitutive model describes the plastic behaviours). Other constitutive material models, e.g. creep models and damage models and so on, can also be conveniently adapted to this inverse approach with suitable adjustments.

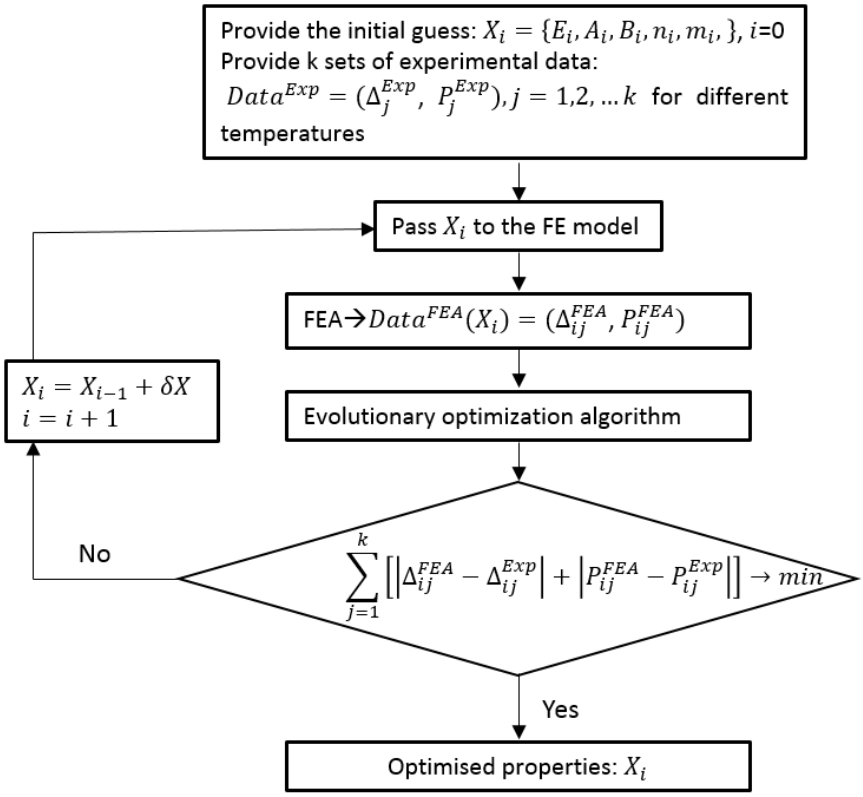

Figure 8. The flowchart of the inverse method.

5.3. Application of the Inverse Approach

The inverse approach was applied for the experimental load-displacement curves obtained from the miniature tensile tests**.** It should be noted that the shape of the experimental curves from 700°C were very dissimilar to those from RT, 500°C and 600°C, e.g. the ductility was significantly higher with a long softening region. The Johnson-Cook constitutive model is more suitable for relatively small strain. Also, damage behaviour was not included by this constitutive model. Therefore, the Johnson-Cook constitutive model was applied to the inverse method for the experimental data obtained at RT and 500°C. According to Eqs (3)-(4), it is clear that the constitutive properties are dependent on the choice of reference temperature. In this case, RT (293K) was selected as the reference temperature, i.e. the constitutive constant *A* was the yield stress at RT.

The evolution of the optimisation function is shown in **Figure 9**. The function value is the measure of the total differences between the predicted load-displacement curves extracted from

FE modelling and the experimental curves. It should be noted that the Johnson-Cook constitutive model does not take account of the temperature effects on the elastic modulus. The elastic modulus was taken as a constant for the optimisation since it is relatively easy to extract the elastic modulus from the experimental results, but certain amount of error might still exist. The comparison between the target curves, initial guess and the optimised load-displacement curves is shown in **Figure 10**. It is clear that the optimised curves are much closer to the experimental curves than the initial guess. The initial guess and the optimised Johnson-Cook constitutive properties are summarised in **Table 2**. Generally, the inverse method was proved to be capable of extracting the Johnson-Cook constitutive properties of the CoNiCrAlY coating using the miniature tensile testing results obtained at different temperatures with very good agreement to the experimental data.

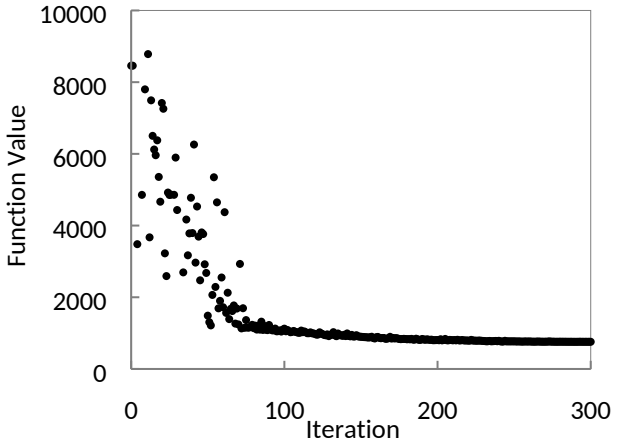

Figure 9. Function evolution of the inverse approach.

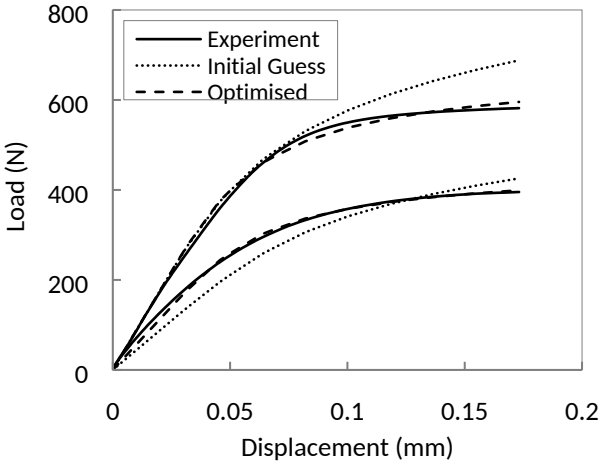

Figure 10. Load-displacement curves: experiment, initial guess and optimised.

Table 2. The initial guess and the optimised Johnson-Cook constitutive properties (RT and 500°C).

	A	*B*	*n*	*m*
Initial guess	700MPa	1000	0.5	0.5
Optimised	765.16MPa	607.18	0.3	1.715

6. Finite Element Modelling of SPT

FE modelling of SPT tests of the CoNiCrAlY coating was carried out using the commercial code Abaqus with the stress-strain behaviour acquired from the miniature specimen tensile tests. The geometry of the FE model was shown in **Figure 11** with the identical dimensions for the SPT tests described in section **2** and section **3.1.** The punch head, the holder, and the die were modelled as axisymmetric analytical rigid bodies. The specimen was modelled as axisymmetric deformable body and meshed using the 4-node bilinear axisymmetric stress quadrilateral with reduced integration elements (CAX4R) and the 3-node linear axisymmetric stress triangle elements (CAX3) for the transition zones. Refined mesh with the elements size 0.02mm was used for the un-supported region of the specimen due to the expected high stress and large deformation.

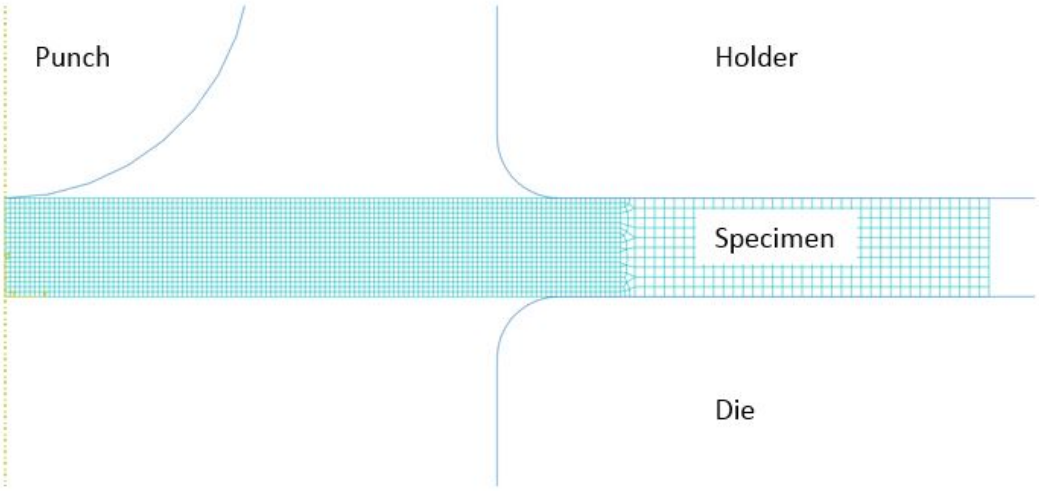

Figure 11. The FE model of SPT Testing.

A failure mechanism was required to characterise the damage evolution of the SPT testing specimen. **Figure 12** shows a typical uniaxial stress-strain curve of a material with (a-b-c-d) and without (a-b-c-d') damage evolution. The fracture energy, i.e. the tensile toughness shown in **Figure 3(b)**, was used for the damage evolution simulation with Abaqus/Explicit. When the energy dissipated in an element reaches the fracture energy value, the element is regarded as failed and removed from the model. As the tensile test proceeds, the global damage evolution is reflected by the increasing number of failed elements removed from the FE model.

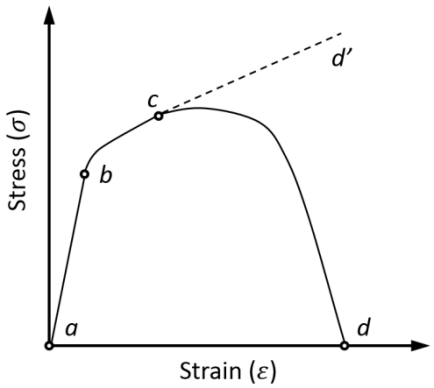

Figure 12. A schematic representation of a uniaxial stress-strain curve of a material with and without damage evolution.

The results of the FE modelling of SPT tests with and without damage evolution compared to the average experimental results are shown in **Figure 13**. It should be noted that the Johnson-Cook properties presented in **Table 2** were used for the FE modelling for RT and 500°C while the estimated stress-strain data was used for 700°C because the material became ductile at 700°C and could not be accurately characterised using the Johnson-Cook model together with RT and 500°C. Generally, at RT and 500°C the maximum load tends to be overestimated when damage evolution is not included while it is predicted closer with damage evolution. More importantly, including damage evolution enables this FE model to predict the early load drops due to cracking found in the SPT tests at lower temperatures as the RT and 500°C curves show.

The damage sites on the SPT specimen are depicted by the removal of the failed elements from the FE model. The comparison between the experimentally observed failure site for the 700°C SPT testing specimen and the corresponding FE modelling contour is shown in **Figure 14.** The FE model was able to predict the failure site to be near the contact boundary of the specimen and the punch head and also predict the circular geometry of the fracture pattern. It should be noted that the current FE model was unable to predict the star-shaped brittle failure pattern observed at lower temperatures shown in **Figure 3(a)**.

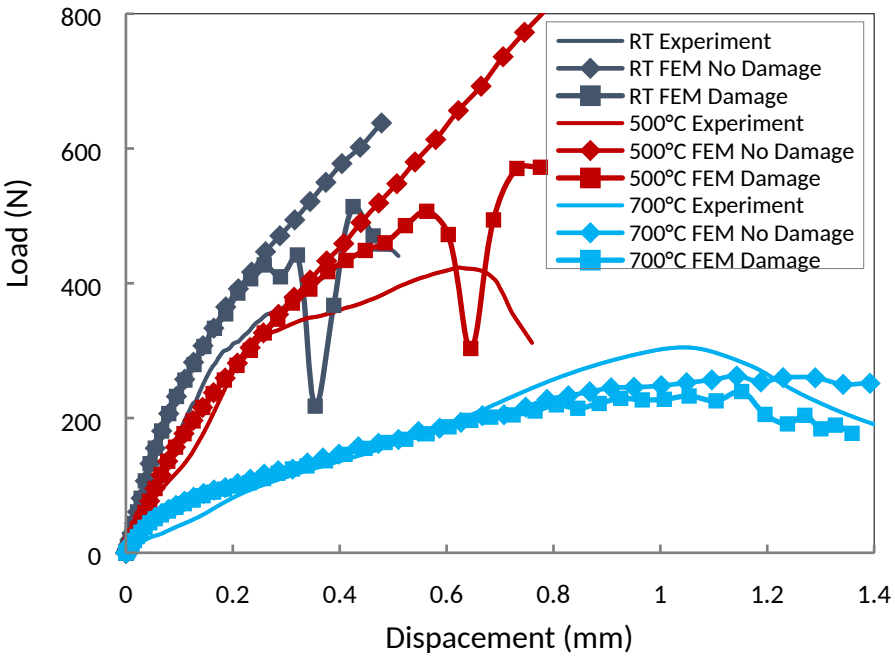

Figure 13. The load-displacement curves: experimental data and FE modelling results of the SPT tests.

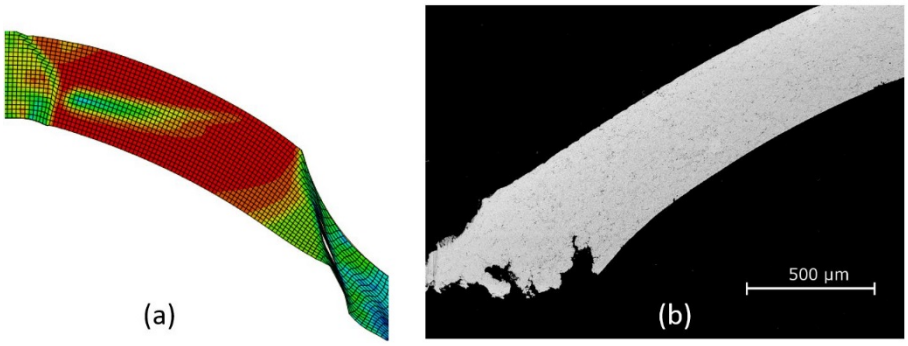

Figure 14. Comparison between the damage sites predicted by FE modelling (a) and observed from the test for the 700°C SPT test.

7. Discussion and Conclusions

Good agreement was achieved regarding the DBTT of the CoNiCrAlY coating between the results obtained from the SPT and miniature tensile tests and a similar experimental study using SPT testing **[9]**, i.e. the DBTT was estimated to be between 600 and 700°C. The repeatability of the SPT tests was very good at 700°C while clear scattering of the results was found at lower temperatures. The consistency and repeatability of the SPT testing at lower temperatures may be compromised by the local heterogeneity of the material, e.g. the random presence of porosity in the specimen, local surface roughness variation and specimen thickness variation, which could have more significant effects on the testing results under the multiaxial stress condition (applied to the SPT testing) than those under the uniaxial stress condition (applied to the miniature tensile testing). Further investigation is needed to verify the possible effects of these potential factors of influence. It was indicated by the results that SPT testing is more reliable as a mechanical testing technique for ductile fracture situations, but less effective for brittle fracture regime for such coatings. Therefore, extra caution should be taken for future SPT testing of brittle materials. The SPT testing results could be improved by applying a consistent clamping force for all tests to reduce possible scattering.

The novel miniature tensile testing method is easier to interpret compared to the SPT testing, i.e. no complex data conversion method is required and the stress and strain could be calculated directly from the measured force, displacement and the specimen geometry, since the deformation mechanisms in the uniform section are similar to those of the conventional uniaxial testing specimens. Although, good comparison of the measured and calculated stress-strain data would make the testing and characterisation method much more convincing. It also eliminates the early load drop, which was found to be a source of data scattering, found in the SPT tests at temperatures lower than the DBTT. The repeatability of the tests was found to be excellent at all temperatures tested. It can be concluded that this novel miniature specimen testing method has demonstrated great potential to become a universally effective mechanical testing technique for both brittle and ductile coating materials in a wide range of temperatures. However, it should be noted that the failure sites of some specimens were near the end of the uniform section, mainly due to the relatively high stress concentration factor (SCF) decided by the specimen geometry (e.g. relatively small fillet radius). Therefore, the testing method can be improved by increasing the radius of the fillet to reduce the SCF to ensure that the fracture occurs within the uniform section of the specimen.

An inverse approach was developed based on the Johnson-Cook constitutive model and applied to characterise the temperature-dependent mechanical behaviour of the coating material using the miniature tensile testing results. The inverse method was proved to be capable of accurately determine the tensile properties of the CoNiCrAlY coating.

FE modelling of the SPT testing was carried out using the constitutive properties obtained using the inverse method and the damage evolution was modelled based on the facture energy values determined from the miniature specimen tensile tests. Comparable predictions were obtained from the FE modelling for the load-displacement curves of the SPT tests, the early load drop in the lower temperature SPT tests (i.e. RT and 500°C) and the circular geometry of the fracture surface observed at higher temperature, i.e. 700°C. The star-shaped fracture pattern observed at lower temperatures could not be modelled by the current FE model.

Acknowledgment

This work was supported by the Engineering and Physical Sciences Research Council (EPSRC) through EPSRC Centre for Doctoral Training in Innovative Metal Process (IMPaCT, www.impact.ac.uk) [Grant Number EPL016206] and the project “Novel High Temperature Steam Transfer Pipes” [Grant number: EP-R000859-1]. The authors would also like to thank Mr. Shane Maskill for his assistance in the experimental work.

References

[1] Bose S. High temperature coatings. Butterworth-Heinemann; 2007.

[2] Evans AG, Mumm DR, Hutchinson JW, Meier GH, Pettit FS. Mechanism controlling the durability of thermal barrier coatings. Prog. Mater. Sci. 2001; 46: 505-553.

[3] Lugsheider E, Herbst C, Zhao L. Parameter studies on high-velocity oxy-fuel spraying of MCrAlY coatings. Surf. Coat. Technol. 1998; 108-109:16–23.

[4] Higuera V, Belzunce FJ, Riba J. Influence of the thermal-spray procedure on the properties of a CoNiCrAlY coating. Surf. Coat. Technol. 2006; 200: 5550–5556.

[5] Chen H, Jackson GA, Sun W. An overview of using small punch testing for mechanical characterization of MCrAlY bond coats. J. Thermal Spray Tech. 2017; 26: 1222-1238.

[6] Tillmann W, Selvadurai U, Luo W, Measurement of the Young’s modulus of thermal spray coatings by means of several methods, J. Therm. Spray Technol. 2013; 22: 290-298.

[7] Waki H, Oikawa A, Kato M, Takahashi S, Kojima Y, Ono F. Evaluation of the accuracy of Young’s moduli of thermal barrier coatings determined on the basis of composite beam theory, J. Therm. Spray Technol. 2014; 23: 1291-1301.

[8] Hyde TH, Sun W. A novel, high sensitivity, small specimen creep test. J. Strain Anal. Eng. 2009; 44: 171-85.

[9] Jackson GA, Sun W, McCartney DG. The application of the small punch tensile test to evaluate the ductile to brittle transition of a thermally sprayed CoNiCrAlY coating. Key Eng. Mater. 2017; 734: 144-155.

[10] Chen H, Hyde, TH, Voisey KT, McCartney DG, Application of small punch creep testing to a thermally sprayed CoNiCrAlY bond coat. Mater. Sci. Eng: A. 2013; 585: 205-213.

[11] Lucas GE, Review of small specimen test techniques for irradiation testing, MTA 1990; 21: 1105-1119.

[12] Chen H, Hyde TH. Use of multi-step loading small punch test to investigate the ductile-to-brittle transition behaviour of a thermally sprayed CoNiCrAlY coating. Mater. Sci. Eng. A. 2017; 680: 203-209.

[13] Eskner M, Sandstro¨m R. Measurement of the ductile-to-brittle transition temperature in a nickel aluminide coating by a miniaturised disc bending test technique. Surf. Coat. Technol. 2003; 165: 71-80.

[14] Workshop Agreement: Small punch test method for metallic materials (Part A), European Committee for Standardization, Brussels, December 2006.

[15] European standard on small punch testing of metallic materials, Bruchhausen M, Austin T et al, American Society of Mechanical Engineers, Pressure Vessels and Piping Division (Publication) PVP, 2017.

[16] Cao L, Bürger D, Wollgramm P, Neuking K, Eggeler G. Testing of Ni-base superalloy single crystals with circular notched miniature tensile creep (CNMTC) specimens. Mater. Sci. Eng. A. 2018; 712: 223-231.

[17] Hafeez Farrukh, Desmukh MN, Husain Asif, Sehgal DK. Miniature test technique for acquiring true stress–strain curves for a large range of strains using a tensile test and inverse finite element method. Applied Mech. Mater. Online 2011; 110-116: 4204-4211.

[18] Kumar Kundan, Pooleery Arun, Madhusoodanan K, Singh RN, Chatterjee Arnomitra, Dutta BK, Sinha RK. Optimisation of thickness of miniature tensile specimens for evaluation of mechanical properties. Mater. Sci. Eng. A. 2016; 675: 32-43.

[19] Hyde TH, Sun W, Williams J. Requirements for and Use of Miniature Test Specimens to Provide Mechanical and Creep Properties of Materials: A Review. Int. Mater. Rev. 2007; 52: 213-255.

[20] Morris A, Cacciapuoti B, Sun W. The Role of Small Specimen Creep Testing within a Life Assessment Framework for High Temperature Power Plant. Int. Mater. Rev. 2018; 63: 102-137.

[21] Wen W, Becker AA, Sun W. Determination of material properties of thin films and coatings using indentation tests: a review. J. Mater. Sci. 2017; 52: 12553-12573

[22] Kang JJ, Becker AA, Wen W, Sun W. Extracting elastic-plastic properties from experimental loading-unloading indentation curves using different optimization techniques. Int. J. Mech. Sci. 2018; 144: 102-109.

[23] Lu J, Campbell-Brown A, Tu Shan-Tung, Sun W. Determination of creep damage properties from miniature thin beam bending using an inverse approach. Key Eng. Mats. 2017; 734: 260-72.

[24] Husain Asif, Sehgal DK, Pandey RK. An inverse finite element procedure for the determination of constitutive tensile behaviour of materials using miniature specimen. Comput. Mats. Sci. 2004; 31: 84-92.

[25] Johnson GR, Cook WH, A constitutive model and data for metals subjected to large strains, high strain rates, and high temperatures. Proc. 7th Int. Symp. on Ballistics, Hague, Netherlands, 1983 April.

[26] Saeidi S, Voisey KT, McCartney DG. The effect of heat treatment and the oxidation behaviour of HVOF and VPS CoNiCrAlY coatings. J. Therm. Spray Tech. 2009; 18:209–216.

[27] Ray AK. Failure mode of thermal barrier coatings for gas turbine vanes under bending. Int. J. Turb. Jet. 2000; 17: 1–24.

[28] Rasche S, Kuna M. Improved small punch testing and parameter identification of ductile to brittle materials. Int. J. Pre. Ves. Pip. 2015; 125: 23-34.

[29] Lancaster RJ, Illsley HW, Davies GR, Jeffs SP, Baxter GJ. Modelling the small punch tensile behaviour of an aerospace alloy. Mater. Sci. Tech. 2017; 33: 1065-1073.

[30] Lacalle R, Alvarez JA, Gutierrez-Solana F. Analysis of key factors for the interpretation of small punch test results. Fati. Frac. Eng. Mater. Stru. 2008; 31:841–928.

[31] Mathworks. Global Optimization Toolbox: User's Guide (r2015a). 2015.